JOURNAL OF APPLIED ELECTROCHEMISTRY **27** (1997) 720–730

Influence of antimony ions and $PbSO_4$ content in the corrosion layer on the properties of the grid/active mass interface in positive lead–acid battery plates

D. PAVLOV, A. DAKHOUCHE, T. ROGACHEV

Central Loboratory of Electrochemical Power Sources, Bulgarian Academy of Sciences, Sofia 1113, Bulgaria

Received 21 January 1996; revised 31 July 1996

Antimony in lead/antimony alloys is known to have a beneficial influence on the capacity and cycle life of lead–acid battery positive plates. The present work shows that $Sb_3O_9^{3-}$ ions formed on oxidation of PbSb alloys improve the capacity of the Pb/PbO_2 electrode, whilst $SbOSO_4^-$ ions have an adverse effect and passivate this electrode. A mechanism of the influence of these ions is proposed based on the gel–crystal concept for the structure of PbO_2. The paper also discusses the effect of $PbSO_4$ formed at the grid/PAM interface on the capacity. It has been established that the major part of the $PbSO_4$ crystals are oxidized to PbO_2 within a few cycles. There still remain a certain number of $PbSO_4$ crystals which border narrow pores and are oxidized at a very slow rate, thus preserving their influence even after 10 discharge–charge cycles. It has also been found that the higher the density of PAM the stronger the adverse effect of $PbSO_4$ in the grid/PAM interface on the capacity. All these phenomena are related to the PCL effect and methods to suppress them are proposed.

1. Introduction

The interface Pb grid/PbO_2 active mass (PAM) consists of two sublayers: the corrosion layer (CL) and the active mass collecting layer (AMCL) [1]. The CL is formed during curing and formation of the plates. This layer grows during battery operation. The AMCL is a thin layer of PAM whose function is to distribute uniformly throughout the active mass the electron flows from the grids during discharge and to collect the current from the PAM and conduct it towards the CL and grid during charge. The above two layers also have a second function, that of a mechanical connection between the grid and PAM capable of dissipating the mechanical stresses that appear on pulsation of the plates during battery cycling. The mechanical and electrical properties of these two sublayers often limit the capacity of the battery and may lead to the so called premature capacity loss (PCL).

The electrical resistance of the grid/PAM interface can be generally represented by Ohm's second law as follows:

$$R = \rho_{CL}\frac{l_{CL}}{S_{CL}} + \rho_{AMCL}\frac{l_{AMCL}}{S_{AMCL}} \qquad (1)$$

where ρ_{CL} and ρ_{AMCL} are the specific resistance of the CL and the AMCL, respectively. l is the thickness of the sublayers and S is the area of crosssection of the solid phases in the interface through which the electronic current flows. S is determined from the expression

$$S_x = S_{grid} - S_{cracks} - S_{pores} - S_{PbO_2/PbSO_4} \qquad (2)$$

S_x is the cross-section area through which the electronic current flows at a distance x from the metal surface. S_{grid} is the grid surface area. S_{cracks} is the effective surface area of the cracks in the CL [2]. S_{pores} is the surface area of the pores at the interface CL/AMCL. The latter depends on the density of PAM. The PAM is built up of PbO_2 agglomerates interconnected into a continuous skeleton and a system of pores formed between the agglomerates of the skeleton. During discharge, part of the PbO_2 at the interface (CL+AMCL) is reduced to $PbSO_4$. The cross-section of the agglomerates in PAM decreases. $S_{PbO_2/PbSO_4}$ accounts for this decrease.

Figure 1 presents the dependence of S_x on the distance from the grid. The smallest cross-section (S_{cr}) through which electrons pass in both directions is that of the interface CL/AMCL that is, the current density in this zone is highest. This interface is the most critical zone in the positive plate. The specific conductivity and the cross-section area of this zone depend strongly on grid alloying additives used, grid and plate design, paste density, current profile on charge and discharge, etc. It is responsible for the PCL effect [1].

Direct investigation of the S_{cr} interface, for example by using a probe to get direct access to this layer, has proved experimentally difficult. Our efforts to reliably incorporate a microsensor into the S_{cr} layer to monitor the changes in its parameters also failed. Thus we used an indirect method to examine the properties of the S_{cr} layer. The positive active mass (PAM) was ground to powder (agglomerates). This PAM powder was filled into tubes with lead

0021-891X

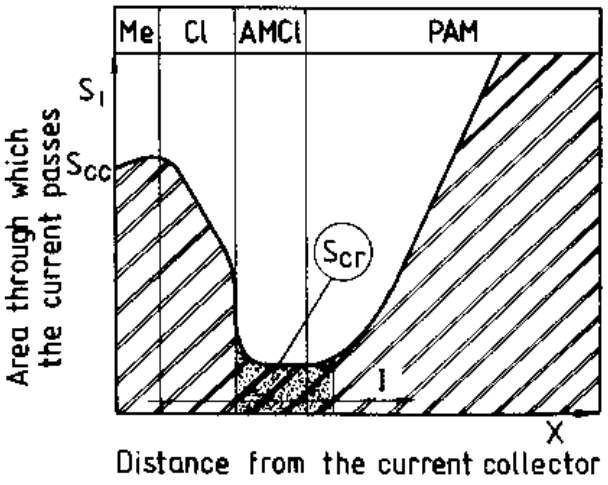

Fig. 1. Scheme of the changes in cross-sectional area parallel to the current collector surface through which current passes with the distance from the current collector (hatched region).

spines in the centre. The spines were covered with CL by anodic oxidation prior to the investigations. Thus a model lead dioxide electrode was fabricated incorporating all parts of a positive plate. When this electrode is subjected to cycling, first the bond CL–AMCL is formed and then the skeleton of PAM. The capacity of this electrode is a measure of the electronic connection between the CL and PAM powder (at the beginning of cycling) as well as between the individual particles in PAM (after 10–15 cycles). In this way the electrode capacity serves as an indirect parameter for the electrical properties of the interface and for the processes of formation of the PAM skeleton. Actually, this is the reverse process to the disintegration of PAM on cycling, which very often limits plate life, but we can assume that these two reverse processes are influenced in a similar way by a given parameter.

The first aim of the present investigation was to study the effect of various antimony ions on the properties of the corrosion layer. This effect had been elucidated earlier for tubular PbO_2 powder electrodes [3, 4]. In this investigation the object of interest was the CL. A comparison between the results obtained in this work with those reported in [4] allow for assessment of the influence of the active mass on the properties of the interface.

Equation 2 contains the terms $S_{PbO_2/PbSO_4}$. The second aim of the present work was to establish how the $PbSO_4$ formed at the interface affects the capacity of tubular powder electrodes and hence the current generation processes in the electrodes.

2. Experimental details

2.1. *Electrode preparation*

Figure 2 shows schematically the construction of the electrodes designed for the investigations with no PAM (Fig. 2a) and with PAM powder (Fig. 2b). The flat electrodes of the type presented in Fig. 2a were used to investigate the corrosion layer. These electrodes were subjected to cycling.

The model tubular powder electrode had the following construction. A lead or lead alloy spine threaded at both ends was inserted into a woven polyester tube which was filled with PAM powder. The polyester tube was plugged at both ends by polyethylene stoppers with threaded apertures in the centre. Through screwing the two stoppers up and down the spine, a definite volume of the tubes was achieved. This volume was filled with PAM powder. Thus, precise control was possible on the density of PAM in the tubular electrode, and, as demonstrated in [3], the PAM density exerts a strong influence on the capacity of the electrode.

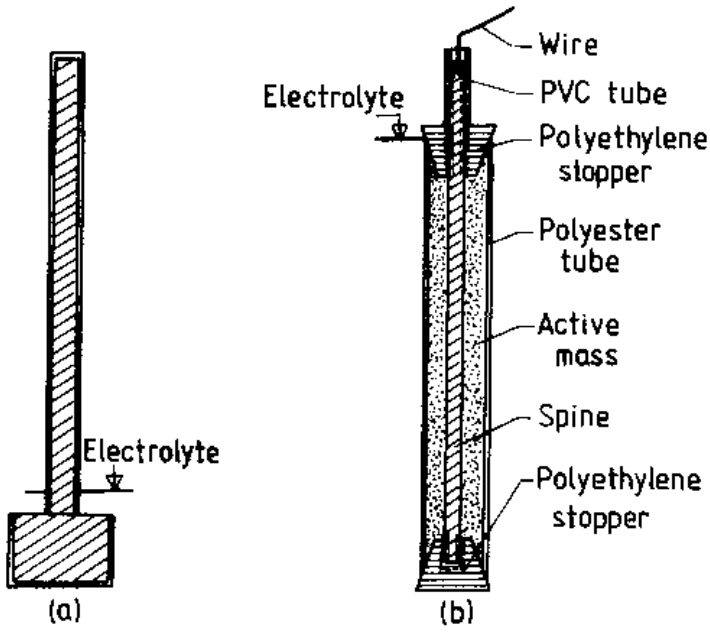

Fig. 2. Working electrodes: (a) used for corrosion layer investigations; (b) tubular powder electrode.

PbO_2 powder preparation: positive and negative plates were produced with pure lead grids. The pastes were prepared at 30–50°C using 6% H_2SO_4/leady oxide ratio. SLI grids were pasted. The plates were subjected to formation in H_2SO_4 with specific gravity (s.g.) 1.15. Cells were assembled and subjected to five charge–discharge cycles at 100% DOD. The positive active mass was removed from the grids, washed with water and dried at 60°C for 2 h. Then it was ground to powder. This PAM powder was filled into the above described tubular electrodes.

2.2. *Cell design*

Cells were assembled with two negative plates with pure lead grids and one tubular or flat lead electrode and one Hg/Hg_2SO_4 reference electrode. The electrolyte used was 4.5 M H_2SO_4 solution. The cells with the tubular electrodes were set to cycling at 15 mA cm^{-2}. The latter current density is often used in lead-acid batteries. The discharge was carried down to 0 V vs the Hg/Hg_2SO_4 reference electrode i.e., the electrodes were fully discharged. The electrodes without PAM were cycled at $i = 4.5$ mA cm^{-2}. The discharge was conducted until the electrode potential reached 0 V (vs $Hg/HgSO_4$ reference electrode). The quantity of electricity passing through the electrode during the subsequent charge was 20% higher than the capacity during the preceding discharge. On completion of the tests the electrodes were taken out of the cells and subjected to XRD and SEM examinations.

2.3. *Preparation of antimony ion solution*

The influence of antimony ions on the properties of the CL was investigated. The solution of antimony ions in 4.5 M H_2SO_4 was prepared through dissolving 1.5 g of metal antimony in 200 ml of concentrated H_2SO_4 on boiling. After cooling of the solution the latter was diluted with water to give a concentration of 1.28 s.g. at 25°C. The oversaturated solution was left for 24 h and then filtered. The obtained filtrate was left for another 24 h and then filtered again. This procedure was repeated until stable and clear solution was obtained. In this way an antimony concentration of 1.30 g dm^{-3} was achieved in the H_2SO_4 solution with s.g. 1.28. Antimony was present in the form of $SbOSO_4^-$ ions in this solution [5].

3. Results

3.1. *Influence of $SbOSO_4^-$ ions in the solution on the properties of the CL*

3.1.1. Lead electrodes. Investigations were performed using solutions with three different antimony concentrations: 10^{-3}, 2×10^{-3} and 10^{-2} M in H_2SO_4 s.g. 1.28. For comparison, experiments with H_2SO_4 s.g. 1.28 containing no antimony ions were carried out as well. Figure 3 illustrates the changes in capacity of the CL formed on lead electrodes as a function of the number of cycles. The Pb electrodes were cycled under the conditions described in Section 2.2. first in H_2SO_4 solution s.g. 1.28 (five charge-discharge cycles) to allow formation of corrosion layer on their surface. Then the H_2SO_4 solution in three of the four cells under investigation was replaced with H_2SO_4 s.g. 1.28 containing $SbOSO_4^-$ ions in the above three concentrations and cycling was continued. The cells were subjected to four discharge–charge cycles daily and then left on charge during the night.

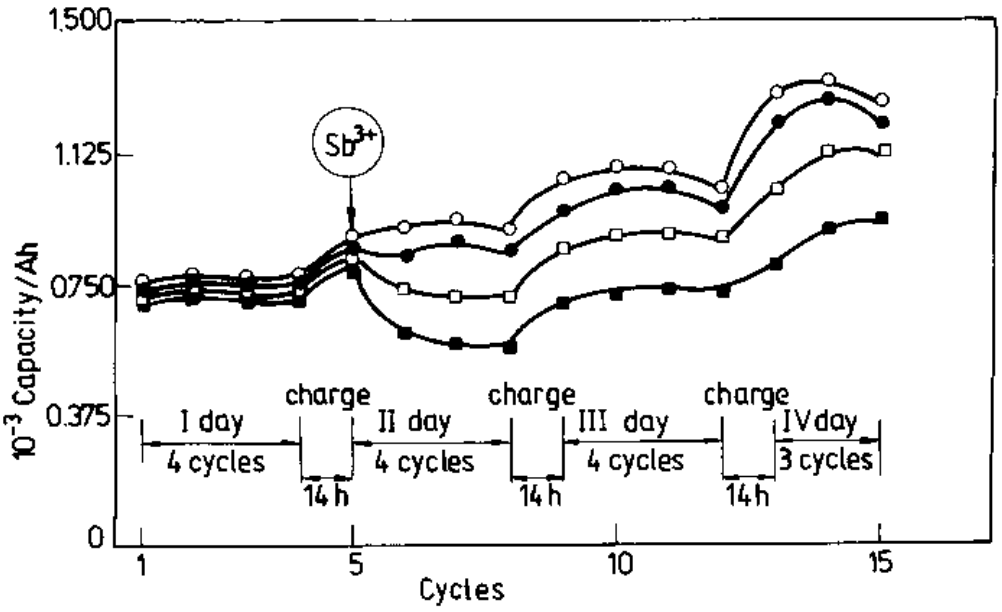

Fig. 3. Dependence of the capacity of the CL formed on lead electrodes on the number of cycles. Antimony ions ($SbOSO_4^-$) are added in different concentrations to the 4.5 M H_2SO_4 solution during the 5th cycle. The uppermost curve refers to a lead electrode cycled in H_2SO_4 solution containing no antimony ions. Key: (○)0 M Sb^{3+}; (●)10^{-3} M Sb^{3+}; (□)2×10^{-2} M Sb^{3+}; (■)10^{-2} M Sb^{3+}.

Figure 3 shows that all electrodes exhibit similar capacities up to the 5th cycle. On addition of antimony ions the capacities decreased immediately. The higher the Sb concentration the greater the capacity decrease. This indicates that $SbOSO_4^-$ ions passivate the lead dioxide electrodes.

On completion of cycling, the electrodes were taken out of the cells and X-rayed without washing the H_2SO_4 solution away. The diffraction patterns were recorded with filtered copper radiation. Figure 4 presents the dependence of the intensities of the characteristic diffraction lines for α and β-PbO_2 on the concentration of antimony ions in the solution.

It can be seen from the figure that $SbOSO_4^-$ ions, even in concentrations of 10^{-3} M, cause a significant decrease in intensity of the characteristic diffraction lines, that is, lead to amorphization of the PbO_2 particles in the CL. This effect of antimony ions has also been observed on immersing PAM in H_2SO_4 solution containing $SbOSO_4^-$ ions [6].

3.1.2. Lead–antimony electrodes. Electrodes produced with lead–antimony spines containing 0.1, 0.8, 2 or 9% Sb in the alloy were also subjected to cycling under the conditions described in Section 2.2. Figure 5 gives the capacities measured after 1, 5, 15 and 17 cycles for the four types of lead–antimony electrodes and for a pure Pb one in H_2SO_4 solution.

During the first discharge, apart from the 0.1 Sb electrode whose capacity decreased, a slight increase in capacity was observed in the other electrodes with PbSb spines. The electrode capacity increased further with cycling. The higher the Sb content in the alloy the greater the capacity increase. It can be assumed that antimony accelerates the anodic oxidation of lead and facilitates the formation of a thick anodic layer. There is a good electronic and mechanical connection between the particles in the CL, which ensures high electrode capacity.

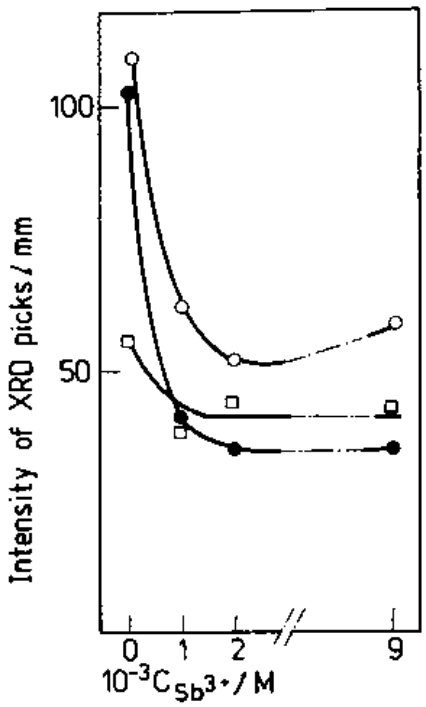

Fig. 4. Intensity of the characteristic diffraction lines for (□) α-PbO_2 (d = 0.312 nm) and (● and ○) β-PbO_2 ($d = 0.350$ nm and $d = 0.279$ nm respectively) in the CL against concentration of antimony ions in the H_2SO_4 solution.

On comparing the data in Figs 3 and 5 it can be seen that the antimony ions formed on oxidation of the PbSb alloys have the opposite effect to that of $SbOSO_4^-$ ions. It has been established that oxidation

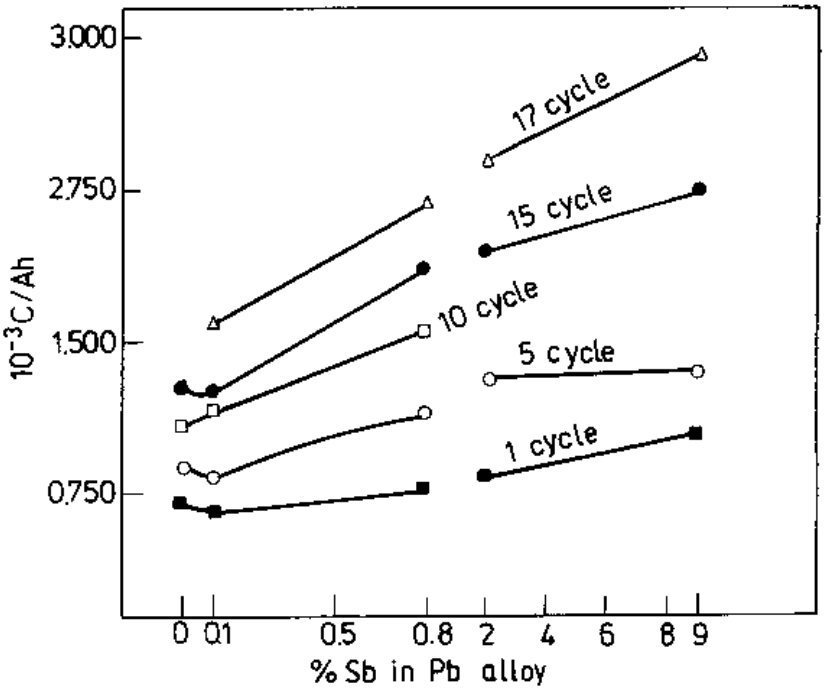

Fig. 5. Capacity of the corrosion layer formed on Pb and PbSb electrodes on cycling in H_2SO_4 solution in dependence of the Sb content in the spine alloy.

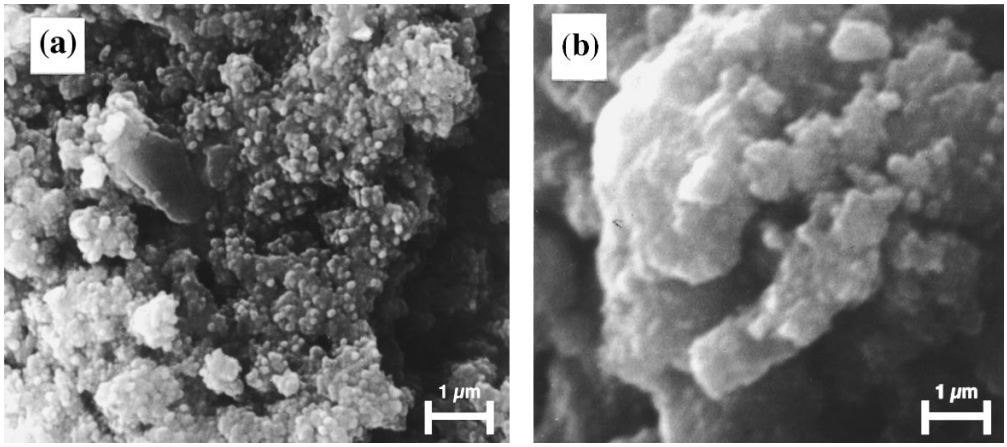

Fig. 6. SEM micrographs of the corrosion layer formed on: (a) Pb–0.1% Sb electrodes; (b) Pb–9% Sb electrodes.

of PbSb alloys in H_2SO_4 solution results in the formation of antimony complexes of the type $Sb_3O_9^{3-}$ [7]. In contrast to $SbOSO_4^-$ ions their $Sb_3O_9^{3-}$ counterparts exert a beneficial effect on the capacity of the electrodes.

Figure 6 presents SEM micrographs of the CL formed on Pb–0.1%Sb and Pb–9% Sb electrodes on completion of cycling.

The CL is built of interconnected agglomerates. The latter consist of smaller hardly differentiated 'particles' or zones. In the CL formed on Pb–0.1% Sb electrodes (Fig. 6(a)), edges and walls can be distinguished. The 'particles' building the agglomerates in the CL on Pb–9%Sb electrodes have rounded gel-like surfaces. The XRD pattern of this CL indicates a highly amorphous structure as compared to the CL formed on Pb–0.1%Sb electrodes.

TEM micrographs of the CL formed on Pb–0.1%Sb and Pb–9%Sb electrodes are shown in Fig. 7.

It can be seen clearly that the CL comprises zones (particles) with different densities. The dark zones have α or β-PbO_2 structure (determined through microelectron diffraction). The light zones and surface layers are amorphous and release water on heating in the TEM microscope. This indicates that they are hydrated. A comparison between the TEM micrographs of particles from the two types of electrodes shows that the CL formed on Pb–9%Sb electrodes has a higher degree of hydration. A similar phenomenon has been observed and described in [8].

3.1.3. Lead–antimony electrodes cycled in H_2SO_4 solution containing antimony ions. Electrodes produced using the four types of PbSb alloys mentioned in Section 1.2. were subjected to cycling in H_2SO_4 solutions containing antimony ions in the concentrations given in paragraph 1.1. These ions were introduced to the solutions after nine cycles and then cycling was continued. Figure 8 presents the capacity curves obtained.

Addition of $SbOSO_4^-$ ions to the H_2SO_4 solution leads always to a decrease in electrode capacity

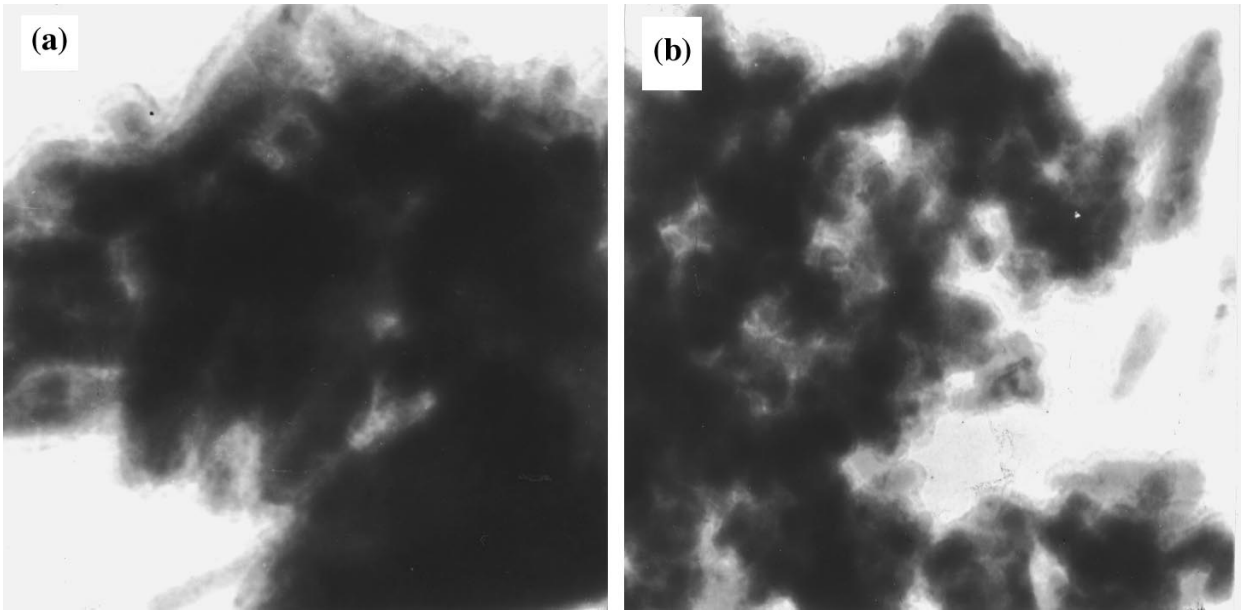

Fig. 7. TEM micrographs of the corrosion layer formed on: (a) Pb–0.1% Sb electrodes; (b) Pb–9% Sb electrodes. Magnification: 150 000 ×.

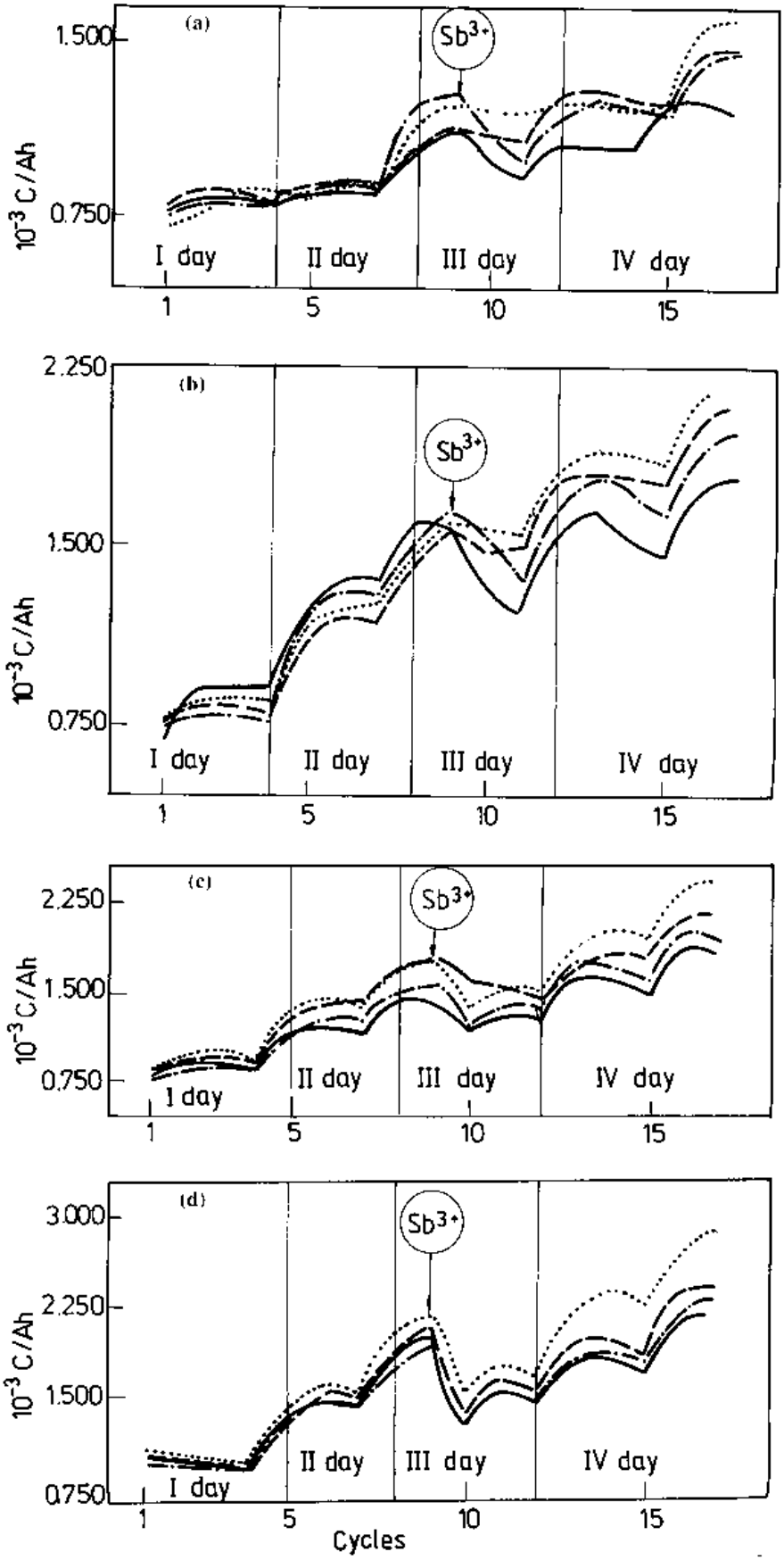

Fig. 8. Capacity against number of cycles curves for the corrosion layers obtained on cycling of PbSb electrodes with different Sb content in the spine alloy immersed in H_2SO_4 solutions containing $SbOSO_4^-$ ions in different concentrations. Key: (·····)H_2SO_4; (– – –)1×10^{-3} M Sb^{3+}; (–·–·–) 2×10^{-3} M Sb^{3+} ; (——)1×10^{-2} M Sb^{3+} for (a) Pb–0.1% Sb, (b) Pb–0.8% Sb, (c) Pb–2% Sb and (d) Pb–9% Sb.

irrespective of the antimony content in the alloy. On comparing the results from Figs 5 and 8 it becomes evident that the beneficial effect of the $Sb_3O_9^{3-}$ ions formed on oxidation of antimony in the alloy is suppressed by the passivating influence of the $SbOSO_4^-$ ions in the solution.

When the Pb–2%Sb and Pb–9%Sb electrodes were cycled in pure H_2SO_4 solution, no shedding of the CL was observed up to the 15th cycle. On adding of $SbOSO_4^-$ ions, however, the CL layer began to shed after several cycles. This means that $SbOSO_4^-$ ions impair the mechanical connection between the PbO_2 particles formed on cycling in the CL.

3.2. *Effect of state-of-charge of the CL on the processes of formation of PAM structure*

It has been established that, on cycling of batteries with Pb–Ca grids, the concentration of $PbSO_4$ crystals near the positive grid increases and the life of the batteries is shortened [9]. Other authors have found that during float service of batteries, a high concentration of $PbSO_4$ is observed around the grid, when the latter is made of PbCa alloys. This phenomenon is not evidenced in PbSnCa and PbSb grids [10]. It has also been established that $PbSO_4$ crystals are formed only in those parts of the corrosion layer which are in contact with PAM [11]. The effect of $PbSO_4$ crystals at the interface CL/PAM on the capacity and the evolution of this effect on cycling of the plates has not yet been completely elucidated. This effect can be assessed using tubular powder electrodes.

3.2.1. Pb and PbSb electrodes. The investigations were performed using electrodes with Pb–6%Sb, Pb–2%Sb and pure Pb spines. Nine electrodes of each type were set to cycling. All electrodes were cycled for nine cycles first to allow formation of corrosion layer. During the last cycle, three electrodes were discharged to 50% of their capacity during the previous discharge. Another three electrodes were discharged fully (100%). And the last three electrodes remained with their corrosion layer fully charged. The spines were taken out of the cells, washed and dried. Then they were used for the manufacture of tubular electrodes with PAM density 4.15 g cm^{-3}. These tubular electrodes were subjected to cycling in H_2SO_4 solution. The first discharge was conducted with no preliminary charge.

The dependences of the specific capacity (in Ah g^{-1} PAM) against the number of cycles for tubular electrodes with 0%, 50% and 100% state-of-charge of the CL are presented in Fig. 9. Each point reflects a mean arithmetic value of the measurements for the three electrodes.

During the first cycle, the electrodes with fully discharged CL exhibit the smallest capacity. Pure Pb electrodes (Fig. 9(a)) 'remember' the state-of-charge of the CL for more than 10 cycles. In electrodes with Pb–2%Sb spines (Fig. 9(b)) the state-of-charge of the CL influences their capacity for about five cycles. After that the difference in capacity diminishes. Moreover electrodes with fully discharged CL have slightly higher capacity than those with CL discharged to 50% state-of-charge. A similar behaviour is also observed in electrodes with Pb–6%Sb spines (Fig. 9(b),(c)).

During discharge the structure of the CL changes. Most probably the bonds between the individual particles in the CL become shorter and the particles decrease in size. The data presented in Fig. 9(a)–(c) indicate that these changes influence the capacity of the electrodes. This influence is less pronounced in lead–antimony electrodes. Figure 9(d)–(f) (which offers another way of presenting the results from Fig. 9(a)–(c)) illustrates this relation most clearly by comparing the capacity/number of cycle curves for Pb and PbSb electrodes with the same state-of-charge of the CL. The pure lead electrodes exhibit low capacity which increases but very slowly. The capacity of PbSb electrodes (irrespective of the state-of-charge of the CL) increases rapidly on cycling, which indicates that the structures of both the AMCL and of PAM are formed very quickly. Within 10 cycles, the specific capacity of tubular electrodes reaches values close to those of the SLI plates from which the PAM powder was produced, irrespective of the state-of-charge of the CL. Obviously, Sb creates conditions for the phenomena proceeding at the interface to become reversible and facilities the oxidation of $PbSO_4$ and the formation and growth of the AMCL and PAM skeletons.

3.2.2. Effect of PAM density. On discharge of the CL its structure changes (i.e., size of agglomerates, cross-section area through the links between them, thickness of the CL, depth of penetration of the H_2SO_4 solution into the CL etc.). It is of interest to elucidate the impact of PAM density on the structure of the interface layers and, consequently, on the capacity of tubular electrodes. To study this effect we investigated tubular electrodes with different states-of-charge of the CL and different PAM densities (3.80 and 4.15 g cm^{-3}). Figure 10 shows results for electrodes with Pb-2% Sb spines.

The greatest difference in capacity between electrodes with charged and discharged CL is observed during the first four cycles. Then this difference diminishes abruptly. However, the effect of the state-of-charge of the CL on the capacity is still noticeable until the 10th cycle. Another interesting finding is that the difference in capacity between the tubular electrodes with fully charged CL and their counterparts with partially or fully discharged CL is more significant for electrodes with PAM density of 4.15 g cm^{-3} than for those with 3.80 g cm^{-3} PAM density. This is due to the ability of the PAM porous system to allow H_2SO_4 and H_2O flow. The flow in dense PAM is impeded and the reduction of $PbSO_4$ in the CL proceeds at a slower rate, that is, $PbSO_4$ remains longer in the CL.

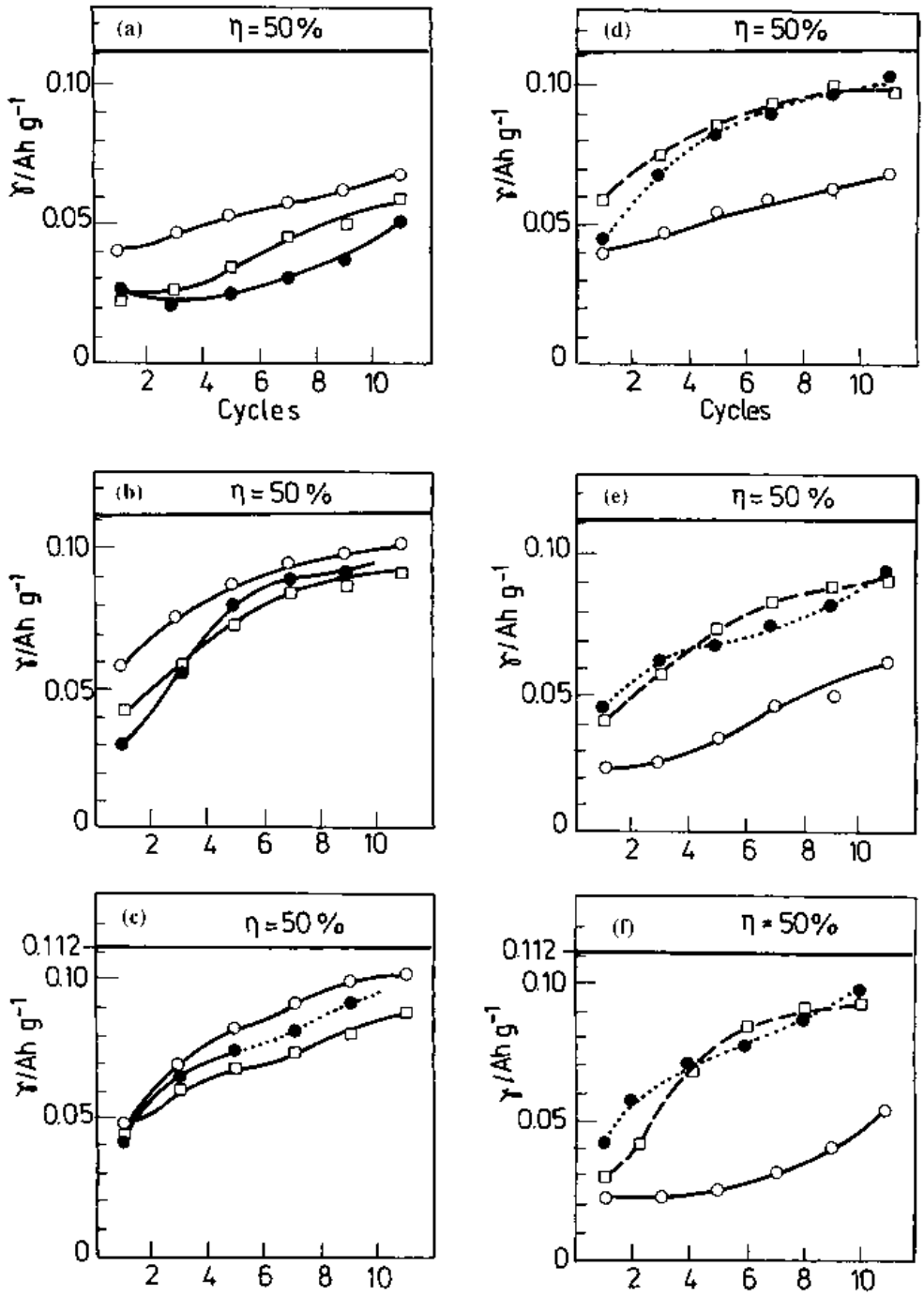

Fig. 9. Changes in specific capacity on cycling of tubular powder electrodes with spines of (a) Pb, (b) Pb–2%Sb and (c) Pb–6%Sb alloys, and (d) 0, (e) 50 and (f) 100% state-of-discharge of the CL. $\eta = 50\%$ means 50% of the theoretically calculated specific capacity. Key for (a,b,c): (●)0% charged, (□)50% charged and (○)100% charged. Key for (d,e,f): (○)Pb, (□)Pb–2%Sb and (●)Pb–6%Sb.

On comparing the specific capacities of electrodes with the two PAM densities it is evident that the density of PAM exerts a stronger influence on the specific capacity than does the $PbSO_4$ content in the CL.

4. Discussion

4.1. *Influence of antimony ions on the properties of the CL*

It has been shown that the PbO_2 anodic layer and PAM tend to adsorb water, as a result of which hydrated zones are formed on the surface of the agglomerates [12–14]. It has been quantitatively determined that PbO_2 in the corrosion layer is about 10% hydrated ($PbO(OH)_2$) when formed on Pb electrodes [8] and contains up to 25% hydrated $PbO(OH)_2$ zones when PbSb electrodes are anodically oxidized [15]. The TEM micrographs presented in Fig. 7 show that not only is the surface of the agglomerates hydrated, but there are also hydrated zones in their bulk. It was assumed that PbO_2 is built of short polymer linear chains [16] and the hydrated zones and layers comprise short hydrated linear polymer chains of the type [17]:

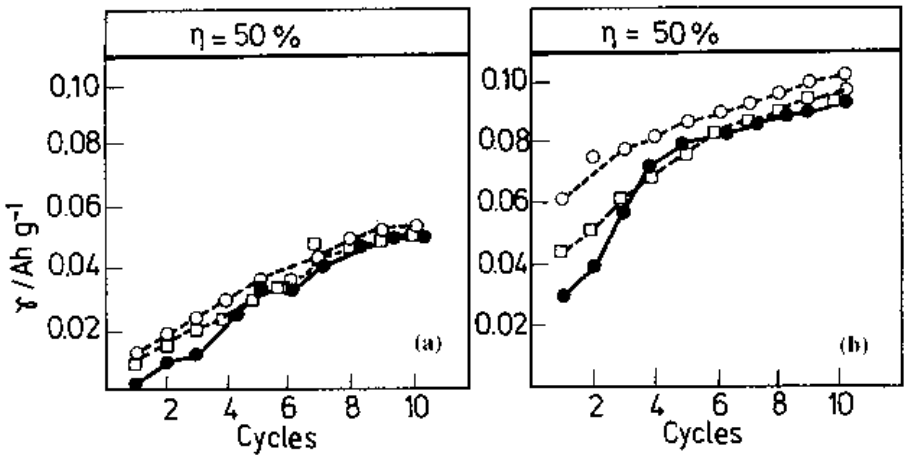

Fig. 10. Changes in specific capacity on cycling of tubular powder electrodes with Pb–2% Sb spines and 0,50 and 100% state-of-discharge of the CL. (a) PAM density $d = 3.80$ g cm^{-3}, (b) PAM density $d = 4.15$ g cm^{-3}. Key: (○)100% charged, (□)50% charged and (●) 0% charge.

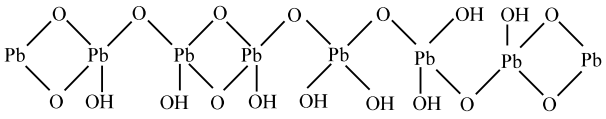

These chains have both electronic and protonic conductivity. The electronic connection between the crystal zones is realized through jumping of electrons from one polymer chain to the other. The hydrated (gel) layers and zones, and the crystal zones in the CL are in equilibrium which can be expressed as follows [6, 17]:

crystal zone amorphous zones

$$PbO_2 + H_2O \rightleftharpoons PbO(OH)_2 \rightleftharpoons H_2PbO_3 \qquad (3)$$

$$\downarrow\uparrow A^- \qquad \downarrow\uparrow K^+$$

where A^- and K^+ are anions and cations in the solution. The ion exchange between the hydrated zones and the solution makes the lead dioxide system an open system [6].

The data presented in Fig. 4 indicate that when the CL is formed in H_2SO_4 solution containing $SbOSO_4^-$ ions, its crystallinity decreases significantly, that is, the CL is strongly hydrated. $SbOSO_4^-$ ions are incorporated into the gel zones and cause a shift to the right of the equilibrium (Reaction 3). Figure 3 shows that a decrease in capacity of the CL is observed in the above case. Based on the gel–crystal structure of the CL the above experimental finding may be explained as follows. Ion exchange of part of the OH^- ions in the polymer chains of the gel zones with $SbOSO_4^-$ ions from the solution proceeds. Consequently, the $SbOSO_4^-$ ions are incorporated into the gel zones of the solid phase and affect the electrical and mechanical properties of the gel zones and layers. As these ions have considerable volume, when incorporated into the chains they increase the distances between them and hence the transfer of electrons from one polymer chain to another is impeded. The electrical resistance of the gel zones increases. As many of the particles formed in the CL on cycling are interconnected through their gel zones, the increased electrical resistance of the gel layers limits the number of particles that take part in the current generation processes, that is, the capacity of the CL decreases. Figure 5 shows just the opposite tendency, namely when antimony is introduced into the spine alloy the capacity of the CL increases.

The anodic oxidation of PbSb alloys in H_2SO_4 solution leads to the formation of $Sb_3O_9^{3-}$ ions [7]. Antimony is in the form of a five-valent ion in this complex. In this case, too, the effect of the $Sb_3O_9^{3-}$ ions can be explained on the basis of the gel–crystal structure of the CL. Each of the above multivalent complex ions is bound to more than one polymer chain. Thus, a polymer network is formed. Electrons do not have to jump from one polymer chain to the other, but move along the polymer network. In this way the conductivity of the gel zones and layers is improved. The electronic contacts between the surface gel layers of the particles are also improved. Consequently, more particles are involved in the current generation process. Thus $Sb_3O_9^{3-}$ ions play the role of a binding element and hence improve the capacity of the CL.

Figure 8 shows that irrespective of the Sb content in the alloy, the capacity of the CL declines on increasing the concentration of $SbOSO_4^-$ ions in the solution. The effect of $Sb_3O_9^{3-}$ ions on the CL formation is weaker than that of $SbOSO_4^-$. Probably $SbOSO_4^-$ ions exchange more readily with OH^- ions in the hydrated polymer chains and have higher affinity towards them than the $Sb_3O_9^{3-}$ ions. This explains why the adverse effect of $SbOSO_4^-$ ions on the capacity of the CL dominates.

The $SbOSO_4^-$ ions incorporated into the gel zones of the CL increase the degree of hydration of these zones, i.e. reduce the concentration of polymer chains in them. Thus, the mechanical bond between the particles in the CL is weakened and they shed easily on oxygen evolution.

Figure 11 presents the specific capacity (at the 20th cycle) of tubular powder electrodes with PbSb spines on cycling in H_2SO_4 solution containing $SbOSO_4^-$ ions in the concentrations mentioned in paragraph

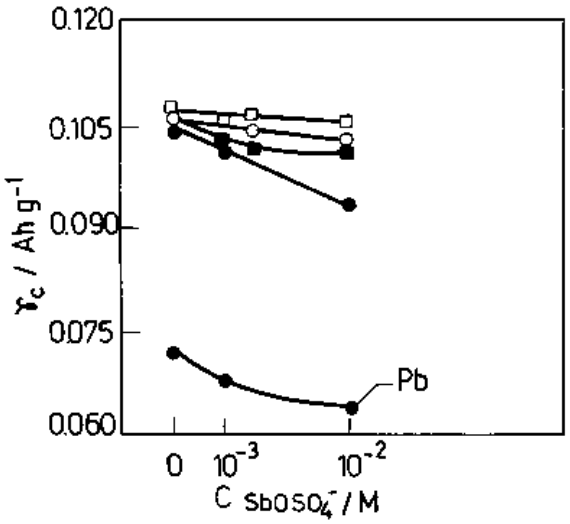

Fig. 11. Specific capacity of PbSb tubular electrodes at the 20th cycle in dependence of the concentration of antimony ions in the 4.5 M H_2SO_4 solution. PAM density, d = 4.15 g cm^{-3}. Key: (□)Pb–6% Sb, (○)Pb–9% Sb, (■)Pb–0.8% Sb and (●)Pb–1% Sb; lower curve (●)Pb.

1.3 above. These results were obtained in an earlier investigation [4]. Figure 11 shows that $SbOSO_4^-$ ions exert the strongest adverse effect only in the case of tubular electrodes with Pb–0.1%Sb spines. In Pb–0.8%Sb electrodes this influence is far less pronounced and in Pb–6%Sb electrodes the adverse effect of $SbOSO_4^-$ ions is suppressed by the beneficial influence of $Sb_3O_9^{3-}$ ions.

Penetration of $SbOSO_4^-$ ions into the pores in PAM is somewhat limited by the diffusion rate. On the other hand, $Sb_3O_9^{3-}$ ions are generated at the interface CL/AMCL and enter the pores of the interface and the PAM. Their movement along the pores is also diffusion limited, as a result of which their concentration in the pores is high. This concentration depends on the Sb content in the spine alloy. In electrodes with higher Sb content, the beneficial effect of $Sb_3O_9^{3-}$ ions on the structure and properties of the gel zones, manifested in the formation of polymer networks, dominates.

Thus, antimony ions have their specific effect on the formation and structure of the CL, AMCL and PAM. Only certain types of antimony ions (in this case $Sb_3O_9^{3-}$) gave beneficial influence on the restoration of the structure of the positive plates and, hence, on battery cycle life.

4.2. *Effect of PAM density on the electrochemical processes at the CL/PAM interface*

The role of the $PbO_2/PbSO_4$ reaction at the CL/PAM interface on the capacity of the plate can be examined by introducing $PbSO_4$ into the CL prior to manufacture of the tubular powder electrode. Thus, through discharge of the CL, $PbSO_4$ crystals are injected only into the CL/PAM interface and the PAM remains charged. The following electrochemical reaction proceeds during charge:

$$PbSO_4 + 2H_2O \rightleftharpoons PbO_2 + H_2SO_4 + 2e^- + 2H^+ \quad (4)$$

For this reaction to proceed the following prerequisites are needed: (i) Good electronic conductivity of the CL and of the AMCL to allow electrons evolved during Reaction 4 to pass from the interface into the grid (spine). For this to happen, the S_{cr} (Fig. 1) should have high electronic conductivity. High PAM density should be used to ensure good electronic contact between the solid phases in the CL and the AMCL. (ii) Good ionic conductivity of the PAM to allow free movement of water and H_2SO_4 ions. This is achieved through a well developed pore system in the PAM. Thus the H_2SO_4 ions and water can move freely between the interior of the PAM and the bulk solution. Hence a low density of PAM is recommended.

Obviously the above two conditions are in contradiction, hence a reasonable compromise must be sought to obtain optimum capacity.

When the density of PAM is low (e.g., 3.80 g cm^{-3}, Fig. 10(a)), a relatively smaller number of lead dioxide particles contact the CL through the gel zones in PAM and the CL particles. These zones, however, have higher electronic resistance than crystal zones. Hence the resistance of the interface is higher and, consequently, the capacity of the tubular electrode is lower (Fig. 10(a)).

When the electrodes have high PAM density (e.g., 4.15 g cm^{-3}, Fig. 10(b)), a greater number of PbO_2 particles are in contact with the CL. The PAM particles contact their neighbours and the CL through their crystal zones or through very dense gel zones. The gel zones with smaller density are pushed away from the contact area. Thus, the electronic conductivity of the interface is improved and the capacity of the tubular electrode during the initial cycles is high. The pore volume in the CL and the AMCL is reduced and the porous system features pores with smaller radii, which decrease the ionic conductivity of the CL. Figure 10 (b) shows that despite the reduced pore volume the capacity of electrodes with PAM density 4.15 g cm^{-3} is higher than that of their counterpart with PAM density 3.80 g cm^{-3}. This indicates that the electronic conductivity during the initial cycles plays a more important role than the ionic transport in the porous system.

Figure 10(a) and (b) shows that the difference in capacity between tubular electrodes with or without $PbSO_4$ in the CL/PAM interface almost disappears within 4–5 cycles. However, even during the 10th cycle part of the $PbSO_4$ remains unoxidized to PbO_2. Probably these $PbSO_4$ crystals are in contact with pores of smaller radii and the diffusion hindrances on the ionic flow, seriously limit the rate of oxidation of the $PbSO_4$ crystals. Thus, the effect of $S_{PbO_2/PbSO_4}$ (Equation 2) is preserved and the electrodes have a slightly lower capacity. In contrast $PbSO_4$ crystals bordering large-sized pores are oxidized for 4–5 cycles and the capacity difference between electrodes with or without $PbSO_4$ in the interface diminishes.

*Table 1. Relative changes in the specific capacity caused by $PbSO_4$ in the CL/PAM interface during the first cycle**

State-of-discharge of the CL /%	γ_r /%	
	3.80 g cm^{-3}	*4.15 g cm^{-3}*
50	29	29
100	86	51

* Data source: Fig. 10 (a) and (b).

4.3. *Influence of PAM density on the reactions of formation and oxidation of $PbSO_4$ in the S_{cr} zone of the CL/PAM interface*

The influence of PAM density on $PbSO_4$ formation and oxidation can be determined from the relative changes in specific capacity (γ_r) of electrodes with 50% and 100% discharged CL (γ_{disch}) as compared to the fully charged CL (γ):

$$\gamma_r = \frac{\gamma - \gamma_{disch}}{\gamma}$$

Table 1 summarizes the first capacity values obtained for tubular electrodes. The data indicate that $PbSO_4$ in the interface CL/AMCL has a more pronounced adverse effect on the specific capacity of electrodes with lower PAM density than on their counterparts with higher PAM density. To avoid this capacity decline the PAM density in the AMCL should be kept high. Thus, the terms $S_{PbO_2/PbSO_4}$ and S_{pores} in Equation 2 are small and the value of S_x is greater. This leads to higher electronic conductivity of the S_{cr}. The high density of PAM in the interface suppresses the phenomena causing PCL.

It is known from battery practice, however, that in order to achieve high PAM utilization coefficient, the PAM pores should have a volume of 0.12–0.14 cm^3g^{-1} PAM. The latter ensures free movement of H_2O and H_2SO_4 along the pores in the plate volume on the one hand and on the other hand the increase in volume of the solid phase resulting from the conversion of PbO_2 to $PbSO_4$ is absorbed and does not cause cracking of the PAM skeleton and of the CL. Hence the ideal positive plate should have highly porous PAM and a dense AMCL layer over the grid.

On cycling of the positive plate the volume of PAM pulsates, expanding during discharge and shrinking during charge. These pulsations are not completely reversible. Consequently, the plate swells and the density of PAM is reduced on cycling. In this process the density of the AMCL may reach such values that the role of $PbSO_4$ becomes crucial. The latter is formed in considerable quantities and hence the term $S_{PbO_2/PbSO_4}$ reaches high values. S_{pores} also increases. As a result of this the term S_x (Equation 2) diminishes. The electronic resistance of the interface S_{cr} (CL/AMCL) increases, which leads to a decrease in capacity of the plate while the PAM is not completely discharged. The life of the battery depends on the rate of the above processes.

To suppress these phenomena, the amplitude of pulsation of the positive plate should be restricted. This may be achieved through (a) confining the volume of PAM (e.g. tubular electrodes); (b) applying pressure to pasted plates during assembly into batteries and (c) formation of a strong PAM skeleton and a well developed pore system to absorb the mechanical stresses resulting from the conversion of PbO_2 to $PbSO_4$ leaving the PAM density unchanged on cycling. Following the above recommendations in positive plate design and manufacture the phenomena leading to PCL would be suppressed thus ensuring longer battery life.

References

[1] D. Pavlov, *J. Power Sources* **53** (1995) 9.
[2] B. K. Mahato, *J. Electrochem, Soc.* **126** (1979) 365.
[3] D. Pavlov, A. Dakhouche and T. Rogachev, *J. Power Sources* **30** (1990) 117.
[4] *Idem, ibid.* **42** (1993) 71.
[5] J. L. Dawson, J. Wilkinson and M. I. Gillbrand, *J. Inorg.Nucl. Chem.* **32** (1970) 501.
[6] D. Pavlov and I. Balkanov, *J. Electrochem. Soc.* **139** (1992) 1830.
[7] J. L. Dawson, M. I. Gillibrand, J. Wilkinson, *in* 'Power Sources 3' (edited by D. H. Collins) Oriel Press, Newcastle-upon-Tyne (1970) pp. 1–9.
[8] B. Monahov and D. Pavlov, *J. Electrochem. Soc.* **141** (1994) 2316.
[9] S. Tudor, A. Weisstuch and S. H. Dowang, *Electrochem. Technol.* **3** (1965) 90; *Ibid* **4**. (1966) 406; *ibid.* **5** (1967) 21.
[10] J. L. Weininger and E. G. Siwek, *J. Electrochem. Soc.* **123** (1976) 602.
[11] S. Hattori, M. Yamashita, M. Kono, M. Yamane, M. Makashima and J. Yamashita, ILZRO Projects LE-253 and LE-276, Ann. Rep. 1978, 1979, International Lead Zinc Research Organization, Research Triangle Park, N C, USA.
[12] J. D. Jorgensen, R. Varma, F. J. Rotella, G. Cook and N. P. Yao, *J. Electrochem. Soc.* **129** (1982) 1678.
[13] R. J. Hill and I. C. Madsen, *J. Electrochem. Soc.* **131** (1984) 1486.
[14] R. J. Hill and M. R. Houchin, *Electrochim. Acta* **30** (1985) 559.
[15] B. Monahov and D. Pavlov, *J. Appl. Electrochem.* **23** (1993) 1244.
[16] G. Kassner, *Arch. Pharm.* **228** (1890) 177.
[17] D. Pavlov, *J. Electrochem. Soc.* **139** (1992) 3075.